Journal of Oil Palm Research Vol. 26 (3) September 2014 p. 251-264

PREPARATION AND CHARACTERISATION OF ACTIVATED CARBON FROM PALM KERNEL SHELL BY PHYSICAL ACTIVATION WITH STEAM

RUGAYAH, A F*; ASTIMAR, A A and NORZITA, N***

ABSTRACT

Granular activated carbon was produced from palm kernel shell using commercial scale carbonisation and activation systems. Carbonisation was carried out using kiln earth system while activation took place in a commercial scale rotary kiln. Steam was used as oxidising agent during activation process with temperature range from 900°C to 1000°C. Palm kernel shell activated carbon was characterised based on proximate and ultimate analyses, thermal stability, chemical functional groups, and surface area. Scanning electron microscope was used to determine the surface morphology of the carbon products. It was found that palm kernel shell is a suitable material to produce activated charcoal owing to its low ash content (2.3 wt %) but high in carbon and volatile content, 23 wt % and 61.7%, respectively. The maximum thermal stability was observed up to 700°C for palm kernel shell activated carbon and raw palm kernel shell but 600°C for palm kernel shell charcoal. The Brunauer-Emmett-Teller (BET) surface area of palm kernel shell activated carbon produced in this study is 607.76 $m^2 g^{-1}$ with 541.76 $m^2 g^{-1}$ micropore area; this is comparable to commercial activated carbon with BET surface area of 690.92 $m^2 g^{-1}$ with 469.08 $m^2 g^{-1}$ micropore area. From the adsorption experiment, palm kernel shell activated carbon could remove up to 80.7% of chemical oxygen demand with 8.83 mg g^{-1} adsorption capacity; this is comparable to the performance of commercial activated carbon available in the market. The results of this study proved that good quality activated carbon can be produced from palm kernel shell.

Keywords: palm kernel shells, physical activation, activated carbon, chemical oxygen demand, palm oil mill effluent.

Date received: 2 October 2013; **Sent for revision:** 6 November 2013; **Received in final form:** 21 May 2014; **Accepted:** 23 June 2014.

INTRODUCTION

Activated carbon (AC) is widely used as adsorbent in the treatment of liquid and gas phases as it contains porous structures, a very important characteristic in an adsorbent. Most of the industrial sectors such as pharmaceutical, mining, petroleum, nuclear, water treatment, food and beverages are using AC in their processing units. The application of AC in such industries is highly demanded due to surface chemistry and unique characteristics of this carbon adsorbent (Rouquerol *et al*., 1998). Basically, the raw materials for AC preparation are mostly coal and pith (Chattopadhyaya *et al*., 2006; Jibril *et al*., 2007; Li *et al*., 2007; Pietrzak *et al*., 2007)

* Faculty of Chemical Engineering,
Universiti Teknologi Malaysia,
81310 UTM Skudai, Johor, Malaysia.

** Malaysian Palm Oil Board,
6 Persiaran Institusi, Bandar Baru Bangi,
43000 Kajang, Selangor, Malaysia.
E-mail: astimar@mpob.gov.my

and recently more focus is directed towards using lignocellulosic by-products as the starting materials. Previous researches had prepared AC from a variety of sources of carbonaceous materials such as coconut shell (Achaw and Afrane, 2008), sawdust (Yadav *et al*., 2013), waste from agricultural activities (Asadullah *et al*., 2006; Cao *et al*., 2006; Cuerda-Correa *et al*., 2008; Deiana *et al*., 2008; Elizalde-González and Hernández-Montoya, 2007; Gerçel *et al*., 2007) and also from agricultural by-products (Bouchelta *et al*., 2008; Lua and Yang, 2005; Nabais *et al*., 2008b; Olivares-Marín *et al*., 2012; Stavropoulos and Zabaniotou, 2005; Sudaryanto *et al*., 2006; Suzuki *et al*., 2007).

The physical characteristics of the AC, such as pore size distribution and pore structure, are commonly used in quantifying the quality of the AC, but these qualities are highly dependent on the nature and the process of the AC preparation. Preparation of AC usually comprises two steps: carbonisation of the raw material in an inert atmosphere to produce charcoal, and followed by physical or chemical activation of the resulting charcoal. The carbonisation process removes the non-carbon elements, such as the hydrogen and oxygen, in the form of volatile gases by pyrolytic decomposition yielding only a rudimentary carbon structure with a fixed mass. This is followed with the activation process to enlarge the pore diameter and also to create new pores and thus enhancing the adsorption properties of the products (Hu *et al*., 2001).

The activation process can be carried out either by physical or chemical means. The common activating agents in physical activation process are carbon dioxide or steam. The physical activation process usually takes place at a higher temperature than the chemical activation process (Ahmadpour and Do, 1997). In the chemical activation process, carbonisation and activation occur simultaneously assisted by chemical activating agents, *i.e.* dehydrating agents and oxidants. The common activating agent used is zinc chloride ($ZnCl_2$). However, chemical activation is less frequently used today due to its potential hazard to the environment. In fact, it is not used to prepare AC for application in food and pharmaceutical products to avoid possible contamination of the end products.

Palm kernel shells (PKS) are generated from oil palm milling process. On fresh weight basis, a fresh fruit bunch (FFB) may contain about 27% palm oil, 6%-7% kernel, 14%-15% fibres, 6%-7% shell and 23% empty fruit bunch materials. In Malaysia, a total of 429 mills were in operation with the capacity to process 101.96 million tonnes of FFB at the end of 2012 (MPOB, 2013). Therefore, 5.61 million tonnes of PKS were generated. Although PKS can be used as boiler fuel with the heating value of 17 MJ kg^{-1}, it can also be exploited to produce higher value products, such as AC.

In this study, PKS AC was prepared using PKS as the starting material. The carbonisation process was carried out using kiln system (Astimar *et al*., 2012), while the activation by using commercial scale rotary kiln. The aim of this article is to characterise the physico-chemical properties of the PKS AC. The results are compared to the AC prepared from different sources and systems.

MATERIALS AND METHODS

Materials

PKS were obtained from FELCRA Berhad, Sungai Melikai Oil Palm Mill, Mersing, Johor, Malaysia. Prior to the process, the shells were first dried under the sun for about 24 hr and turned occasionally to remove moisture. While palm oil mill effluent (POME) were collected from MPOB Palm Oil Mill Technology Centre (POMTEC), Labu, Negeri Sembilan, Malaysia.

Carbonisation of PKS

About 1.5 t of PKS was fed into 36 open-head steel cylinder drum (880 mm tall x 610 mm diameter) and all the steel drums were arranged in the closed-system brick kiln (*Figure 1*). The PKS were carbonised inside the kiln for eight days. The temperature was raised from room temperature to 1000°C in controlled atmosphere using firewood as fuel. Additional firewood was placed in the kiln after 24 hr and the kiln was sealed for four days; this stage is known as 'self-burning stage'. The temperature was measured using a set of thermocouple with data logger and the temperature was maintained using input of wood fuels. On the eighth day, the door of the kiln was opened to cool the charcoal. The resulting char was collected, weighed and then ground and sieved to size between 1.0 mm and 2.0 mm.

Activation PKS in Steam

The activation of PKS charcoal was carried out using rotary kiln with the dimension of 17 m long and 2.14 m diameter. The temperature was adjusted to 900°C to 1000°C using diesel burner under the flow of steam as an oxidising agent (*Figure* 2). The steam was applied by the steam generator via a pipe inserted through the rotary kiln. The final product

Figure 1. Charcoal kiln system for this study.

Figure 2. The rotary kiln for the activation process.

was collected at the end of 12 hr activation process. The AC was washed with hot distilled water followed by cold distilled water until pH of about seven was reached.

Characterisation of PKS AC

The proximate analysis of raw PKS, PKS charcoal and PKS AC were determined following the ASTM Method D3172 - 07a. The ultimate analyses of the prepared PKS AC were analysed using Elemental Analyser Vario EL III, while oxygen content was analysed using FISON CHNS-O analyser.

Fourier transform infrared (FTIR) spectroscopy model Spectrum One by Perkin Elmer was used to identify the functional groups of raw PKS, PKS charcoal and PKS AC. The ranges of the wave number of 4000 to 600 cm^{-1} were recorded.

Thermal behaviours of the raw PKS, PKS charcoal and PKS AC were studied using thermo gravimetric analyser (TGA), Perkin Elmer 4.0 at temperature range of 30°C to 800°C. The sample was heated at a rate of 20°C min^{-1} under nitrogen gas flow of 20 ml min^{-1}.

The surface structure of the AC samples was determined from the micrograph obtained from the scanning electron microscope (SEM) model Hitachi S3400N. The magnification of the SEM was fixed at 6500X.

The surface area and porosity was determined by nitrogen adsorption at -196°C with an accelerated surface area and porosimetry system (ASAP-2000, Micromeritics). The BET surface area was calculated from the adsorption isotherms by using the Brunauer- Emmett-Teller (BET) equation. The cross-sectional area for nitrogen molecule was assumed to be 0.162 nm^2 and the single total pore volume for the samples was measured from the amount of nitrogen adsorbed at the relative pressure of 0.99.

The adsorption properties of the AC was studied by using palm oil mill effluent (POME). A conventional jar apparatus (VELP SCIENTIFICA model FS6S) was used to adsorb the organic matter in POME. This apparatus could accommodate six beakers and can be simultaneously stirred at the same speed with six spindles of six paddles. The adsorption of the organic matter measured as chemical oxygen demand (COD) was performed to compare the adsorption capacity of PKS AC and commercial AC (CAC), where COD is a measure of the oxygen required to degrade the organic matter present in wastewater. The COD of the treated POME was determined by colorimetric method using HACH colorimeter model DR 890. The test method consisted of the use of HACH vials containing dichromate reagent as chemical oxidant for measuring COD in the range of 0-1500 mg $litre^{-1}$.

As for the adsorption test, 250 ml of POME was placed in a 500 ml flask in the jar test and a known amount of adsorbent was added. The influence of adsorbent dosages (10-125 g) agitated at 150 rpm for 24 hr at pH 7.9 (as received before discharged) was studied for COD removal in treated POME. The calculation of the amounts of adsorption of organics in terms of COD removal onto prepared PKS AC and CAC was based on removal percentage (Equation 1) and adsorption capacity (Equation 2).

$$\text{COD removal (\%)} = (C_0 - C_e) \times 100 / C_0 \quad (1)$$

$$\text{Adsorption capacity (mg g}^{-1}) = (C_0 - C_e)\, V / m \quad (2)$$

where C_0 and C_e represent organic concentrations in POME at initial and equilibrium conditions, respectively. *V* is the volume of POME and *m* is the mass of adsorbent added. For the comparison in the efficacy test, CAC from Sigma Aldrich in granular type (8-20 mesh size) was used.

RESULTS AND DISCUSSION

Chemical Analysis of PKS, PKS Charcoal and PKS AC

The ultimate and proximate analyses of the PKS, PKS charcoal and PKS AC are recorded in *Table 1*. The results showed that the contents of carbon, hydrogen, oxygen and nitrogen in PKS were consistent to those reported for other lignocellulosic materials, such as the cherry stones with C:H:O of 49%:6.37%:44.5%, respectively (Olivares-Marín *et al*., 2012). The results were also comparable with coffee endocarp waste residue with C: H: O of 47.3%: 6.4%: 37.7%, respectively (Nabais *et al*., 2008a).

As far as the proximate analysis is concerned, the contents of moisture, volatile matter, ash and fixed carbon are similar to the values reported for other types of waste, *i.e.* moisture, 8.7%; volatile matter, 62.4%; ash, 1.3%; fixed carbon, 27.6% (Demirbaş, 1999). The starting material with low inorganic matter and ash content is mostly desired because the inorganic components become concentrated progressively in the resulting char and in the final product during the carbonisation process. Moreover, the starting materials with low inorganic and ash content indicate high purity of the carbon material (Matos *et al*., 2011). The moisture content is mostly dependent on the storage conditions such as temperature, weather and humidity. In addition, the functional groups, such as hydroxyl groups (-OH) on the surface of the raw material and the resulting AC could make hydrogen bonding with water and thus increasing the moisture content of the materials.

Fourier Transform Infra-red Analysis

FTIR is a qualitative technique normally used to study the surface chemical functional groups on the activated carbon. The natural black appearance of carbon enables it to absorb almost all of the radiation in the visible spectrum. FTIR spectra usually consist of a variety of peaks which represent the sum of the interactions of different types of groups available in the sample. FTIR spectra for raw PKS, PKS charcoal, and PKS AC are listed in *Table 2*.

The FTIR spectra of raw PKS, PKS charcoal and PKS AC are clearly illustrated in *Figure 3*. Raw PKS,

TABLE 1. PROXIMATE, ULTIMATE AND LIGNOCELLULOSIC ANALYSES OF RAW PALM KERNEL SHELL (PKS), PKS CHARCOAL, AND PALM KERNEL SHELL ACTIVITED CARBON (PKS AC)

Analysis		Raw PKS	PKS charcoal	PKS activated carbon
Proximate analysis (wt%)	Volatile matter	61.7	10.27	10.81
	Ashes	2.3	4.95	2.56
	Fixed carbon	23	82.79	83.07
	Moisture content	12.7	1.98	3.56
Ultimate analysis (wt%)	C	48.9	76.05	82.81
	H	5.21	3.37	4.10
	N	0.07	0.94	2.85
	S	0.19	0.40	0.12
	O	45.63	7.04	10.13
	H/C ratio	0.1065	0.0443	0.050
Lignocellulosic analysis (wt%)	Cellulose	27.7	-	-
	Hemicellulose	21.6	-	-
	Lignin	44	-	-

TABLE 2. FOURIER TRANSFORM INFRA-RED (FTIR) SPECTRA OF RAW PALM KERNEL SHELL (PKS), PKS CHARCOAL AND PKS ACTIVITED CARBON (AC)

Material	Wave numbers (cm^{-1})	Description
Raw PKS	3347	Stretching of O-H in hydroxyl groups and adsorbed water
	2932	CH_2 symmetric stretching
	1606	Very strong aromatic ring stretch, aromatic C-O stretch, phenyl propanoid polymer, aromatic skeletal vibrations plus C=O stretch
	1504	Semi-circle ring stretching in aromatic lignin
	1452	C-H deformation (methyl and methylene) in hemicellulose and lignin
	1240	Weak C-O stretching in hemicellulose
	1032	C-O, C=C, and C-C-O vibrational stretching
PKS charcoal	3347	Stretching of O-H in hydroxyl groups and adsorbed water
	2508	C-H stretching
	1426	C=C stretching vibration of the aromatic ring
	1016	Alcohol groups R-OH
PKS AC	3347	Stretching of O-H in hydroxyl groups and adsorbed water
	1575	C=C stretching vibration of the aromatic ring
	1133	Alcohol groups R-OH

PKS charcoal and PKS AC exhibited very different infra-red spectra as raw PKS had a wide range of strong absorption while the absorption of PKS charcoal and PKS AC was very weak. The strong absorption of raw PKS indicated that a large amount of organic and inorganic matters were available in the sample. These organic and inorganic matters came from cellulose, hemicellulose and lignin as raw PKS was a lignocellulosic compound. On the other hand, the absorption bands of PKS charcoal and PKS AC were nearly flat indicating that almost all of the lignocellulosic materials were completely decomposed during carbonisation and activation processes.

PKS charcoal showed a progressive decrease of oxygen groups as higher temperature was applied. The spectrum of PKS charcoal was nearly flat suggesting that the carbonaceous materials were graphitising under the action of temperature around 1000°C or higher (Gomez-Serrano *et al*., 1996). It is suggested that the graphitised materials do not show infrared bands because there are no changes in dipole moment when the atoms vibrate in the symmetrical crystal buildup of equal atoms

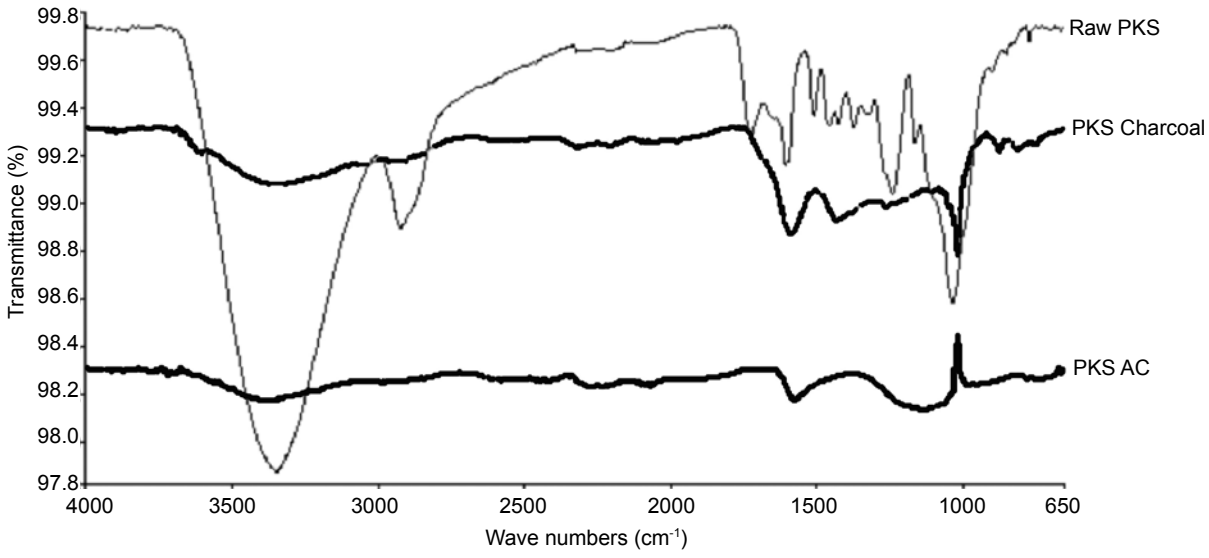

Figure 3. Fourier transform infra-red (FTIR) spectra of palm kernel shell (PKS), PKS charcoal and PKS activated carbon (AC).

(Stuart, 2005). However, Mattson and Mark (1971) reported that some amplified spectrum of graphite had displayed absorption bands in the region of stretching at C=O and aromatic stretching at C=C vibrations.

The three spectra of raw PKS, PKS charcoal and PKS AC displayed the peak at 3347 cm^{-1} and it was associated with vibration in hydroxyl groups (O-H). The location of hydrogen bonded OH groups is usually in the range of 3200-3750 cm^{-1} for alcohols and phenols involved in hydrogen bonding, and this might be attributed to adsorbed water (Chen *et al*., 2002). In addition, certain peaks in raw PKS almost disappeared after carbonisation and activation; this was due to the complete decomposition of the functional groups. Band intensity for PKS AC showed that most of the surface functional groups were present, such as alcohols and phenols. Alcohol groups are typical acidic functional groups. These acidic surface functional groups are favourable for removal of COD (Guo and Lua, 2003). The result obtained for raw PKS showed similarity with other agricultural waste such as rockroses (Gomez-Serrano *et al*., 1996), peach stones (Arriagada *et al*., 1997) and also palm solid waste (Guo and Lua, 2000).

Thermal Analyses of Raw PKS, PKS Charcoal and PKS AC

The thermal analyses of the prepared PKS AC, PKS charcoal and the raw PKS were performed to examine their decomposition characteristics and the TGA curves are as shown in *Figure 4*. Basically, four stages of weight loss occurred in raw PKS and these were at temperatures of: (i) 28.95°C to 150°C, (ii) 150°C to 400°C, (iii) 400°C to 700°C, and (iv) 700°C and above. The first 9.3% weight loss in raw PKS was in between 28.95°C and 150°C; this was due to the elimination of moisture content from the raw sample. During the second stage, at the temperature of 150°C to 400°C, the weight loss was the highest at 49.25%. This very significant weight loss may be due to the removal of volatile matters and less stable constituents of raw PKS that decompose thermally. This also indicates that the pyrolysis process has taken place at this temperature range. The solid black residue obtained at 400°C was basically a carbonised product instead of chars, with an incomplete carbonisation stage. PKS charcoal contained only 0.59 wt% moisture, suggesting that the moisture was totally removed during carbonisation process. At the third stage in the temperature of between 400°C and 700°C, 11.86% weight loss could be detected. At this stage, the volatile matter elimination still continued. The gases released mainly consisted of carbon monoxide (CO) and carbon dioxide (CO_2). The CO resulted from the decomposition of phenols, carbonyl, and quinone groups, and CO_2 from carbonyl groups (Moreno-Castilla *et al*., 1995). With the increase in treatment temperature, the degree of aromaticiy and the fixed carbon content also increased in the resulting carbonised products. In the final stage, at the temperature of 700°C and above, all the carbon matter continued to decompose and at 740°C, the raw PKS had totally been converted into charcoal. No noticeable weight loss could be detected in PKS charcoal during the temperature range between 200°C to 600°C, and for PKS AC up to 700°C.

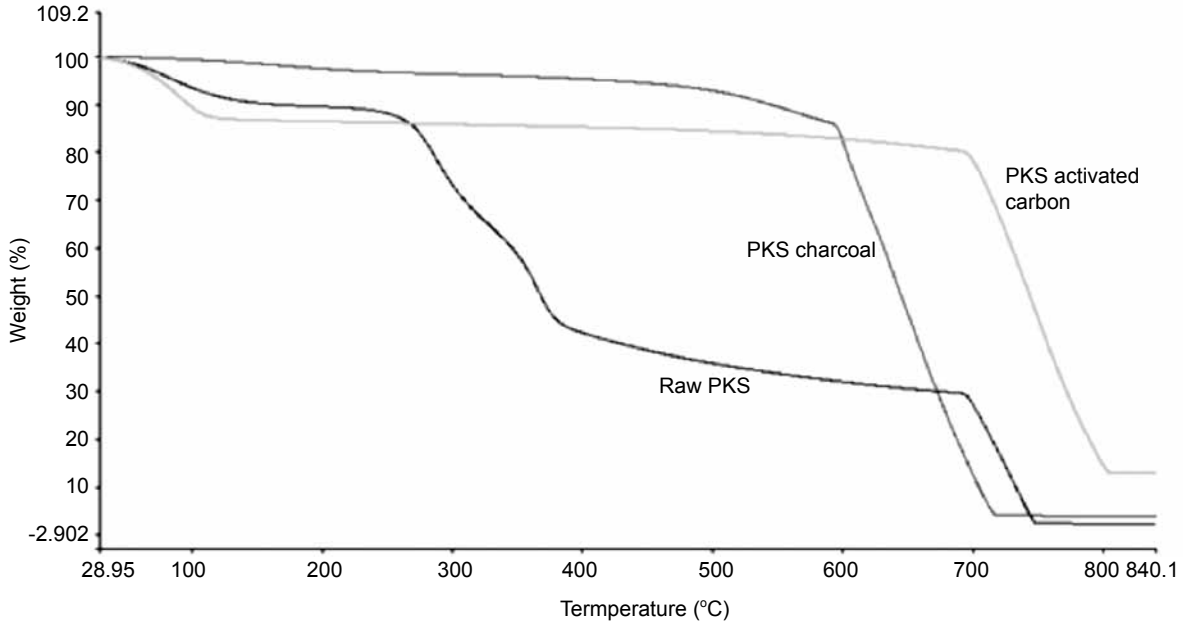

Figure 4. Thermo gravimetric analyser(TGA) profiles of raw palm kernel shell (PKS), PKS charcoal and PKS activated carbon.

In this case, the volatile content of both samples was almost completely eliminated during carbonisation and activation processes. The transformation of the raw PKS into ashes occurred at 600°C while PKS charcoal and PKS AC turned to ashes at 700°C. The plateau line at temperature of over 800°C for all samples showed that the weights were unchanged at the final stage, leaving only ash residues.

The lignocellulosic components for PKS, as shown in *Table 1*, consist of 27.7 wt% of cellulose, 21.6 wt% of hemicellulose and 44 wt% of lignin. The result is in agreement with Daud and Ali (2004). Each component exhibits different thermal behaviours and different products will be generated under thermal decomposition. All these components will decompose from solid to vapour at ascending temperature. Among these three components, hemicellulose is the most reactive and the first to volatilise at the lowest temperature in the range of 225°C and 325°C. In the temperature range of 325°C to 375°C, cellulose will decompose gradually as it has intermediate reactivity. This is then followed by lignin at temperature starting from 250°C and will completely decompose at 500°C; lignin is the most stable component among these three (Sjöström, 1993).

Basically, when cellulose and hemicellulose decompose in elevated temperature, low molecular weight products will be produced. The decomposition of hemicellulose and cellulose produces low molecular weight products commonly comprise of anhydro-sugar, aldehyde, hydroxyl, furan, acetic acid and the carbonaceous chars. On the other hand, when lignin decomposes in elevated temperature, unsaturated chain and phenolics compounds with higher molecular weight, such as eugenol, styrene, alcohols, and carbonaceous chars will be produced. Considerable amount of water will be present in all the products of each component due the common dehydration process before thermal decomposition takes place (Meier *et al*., 2008).

Scanning Electron Microscopy (SEM) Analysis

The surface morphology of raw PKS, PKS charcoal, and PKS AC were examined using SEM. *Figure 5* shows the micrograph of raw PKS analysed at the magnification of 6500X which exhibits the surface of raw PKS. The surface consisted of botanical pores which seemed to have irregular arrangement and some of these pores were unusually large. These pores would provide a template for the development of macropore in the resulting chars (Jia and Lua, 2008). PKS charcoal surface area showed a perfect canal structure indicating that the carbonisation was well developed, but not the activation process (Sun and Jiang, 2010). The AC was obtained by exposing the resulting char to steam activation at 1000°C. Tar-like deposits were obvious on the surface of PKS charcoal (*Figure 6*) but almost clear in PKS AC (*Figure 7*). Most rudimentary pore structure of PKS charcoal was completely blocked with tar-like deposits. According to Rios *et al*. (2006), these tar-like deposits are the products from thermal decomposition and they have migrated from the internal structure of

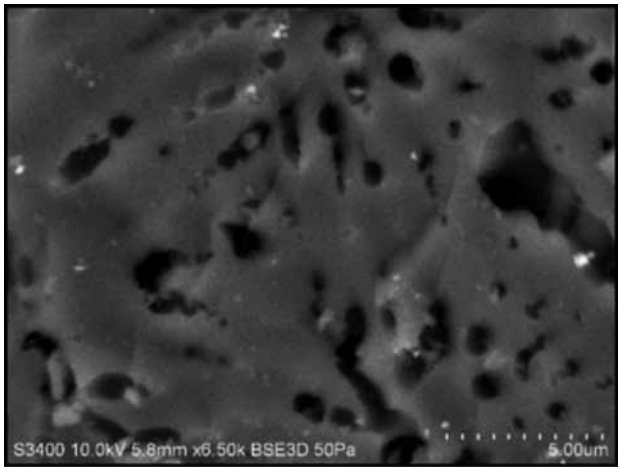

Figure 5. Scanning electron microscopy (SEM) micrograph of raw palm kernel shell (PKS) (6500 X).

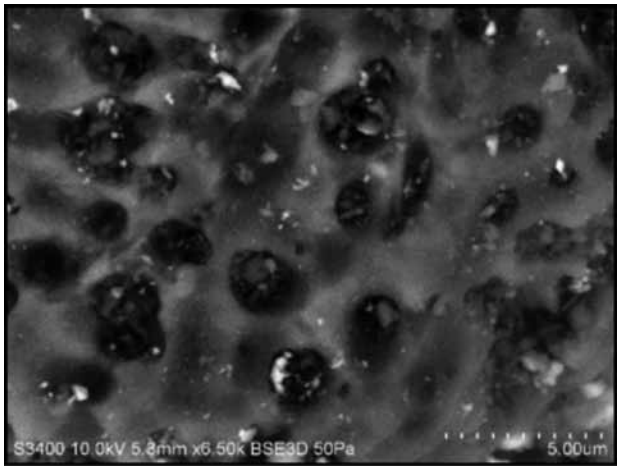

Figure 6. Scanning electron microscopy (SEM) micrograph of palm kernel shell (PKS) charcoal (6500 X).

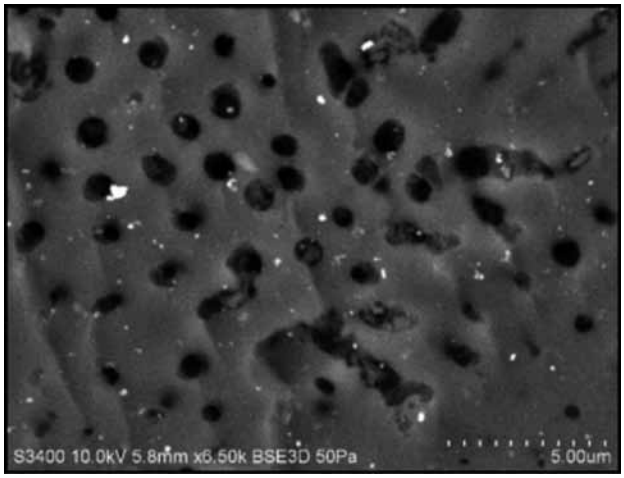

Figure 7. Scanning electron microscopy (SEM) micrograph of palm kernel shell activated carbon (PKS AC) (6500 X).

the chars. The surface of PKS AC in *Figure 7* shows a well-developed rudimentary porous structure with regular pore sizes and cavities which indicate that activation has taken place (Durán-Valle *et al*., 2005). Almost all the canal-like shape developed during carbonisation was eroded by the steam vapour during the activation stage.

Surface Area Analysis

Among the characteristics of the AC, surface area is the most important property as its adsorption capacity is related to the specific surface area (Noll *et al*., 1992). The determination of the adsorption-desorption nitrogen isotherms was carried out at the temperature of 77K using a surface area analyser (Micromeritics ASAP 2020). The surface area analysis of the raw PKS, PKS charcoal, and PKS AC estimated from these isotherms are collated in *Table 3*. Raw PKS gave only 0.72 $m^2 g^{-1}$ of BET surface area, after the activation has been carried out; the BET surface area has increased to 607.76 $m^2 g^{-1}$ with the pore volume of 0.25 $cm^3 g^{-1}$ for the PKS AC. This value is comparable to that of the commercial activated carbon (CAC) with 690.92 $m^2 g^{-1}$ BET surface area and 0.42 $cm^3 g^{-1}$ of pore volume. In particular, CAC consists of 469.08 $m^2 g^{-1}$ micropore area with 221.84 $m^2 g^{-1}$ mesopore area occupying 0.194 $cm^3 g^{-1}$ micropore volume. Prepared PKS AC consists of 541.76 $m^2 g^{-1}$ micropore area and 66 $m^2 g^{-1}$ of mesopore area with 0.21 $cm^3 g^{-1}$ micropore volume. From the result, it can be concluded that PKS AC produced in this study has dominant micropore surface area rather than mesopore area. *Figure 8* shows the nitrogen adsorption-desorption isotherm for both PKS AC and CAC. The shape of the adsorption-desorption isotherm can provide qualitative information on the adsorption process and the degree of the surface area available to the adsorbate. According to the international IUPAC classification of adsorption isotherm, the results obtained for both AC are type 1 indicating that they have micro-porous structures. Pore development in AC is due to the release of volatile matters during the carbonisation and activation processes. However, when compared to other research work on PKS with BET surface area of 973 $m^2 g^{-1}$ and 78 $cm^3 g^{-1}$ total pore volume, the surface area obtained in this study is considered low. Nevertheless, it is worth to mention here that most of the AC production studies were done at the laboratory scale where all the parameters can be well monitored and controlled. These parameters are more difficult to control when studies are conducted at the pilot plant or commercial scales. Low BET surface area obtained also might be affected from the production of inhibitor during activation. During the activation process, the activation gas will come in contact with the char and react with the exterior and diffuse into the interior surface of the particle. The reaction of the chars and water molecule will produce CO and H_2. These products could act as inhibitor in the interior part of the chars. As the concentration of these products increases in the interior part, the reaction of steam at the exterior part will also increase causing the porosity to destruct thereby decreasing its surface area (Rodríguez-Reinoso *et al*., 1995). However, Lartey *et al*. (1999) stated that typical surface area of AC ranges from 500 to 1400 $m^2 g^{-1}$.

Adsorption of Organic Matter Measured as COD

Effect of adsorbent dosage on COD removal. The efficiency of AC in POME polishing treatment was tested by using batch adsorption experiment. AC dosage ranging from 1.0 to 125.0 g of carbon in 250 ml of POME was selected in this experiment. Here, the treatment time was kept constant at 24 hr. Equilibrium was reached corresponding to 20 g/ 250 ml of adsorbent dose for both PKS AC and CAC. The maximum percentage of COD removed from POME was noted as 80.7% and 81.5% for PKS AC and CAC, respectively (*Figure 9*). The initial COD concentration of the untreated POME was 1032 mg $litre^{-1}$ and the final COD concentration obtained after treatment was 199 mg $litre^{-1}$ for PKS AC and 191 mg $litre^{-1}$ for CAC. The increased removal at high dosages is expected because of the increased surface area and availability of the adsorption site at the activated carbon (Garg *et al*., 2003; 2004). *Table 4* lists the comparison of the maximum COD removal

TABLE 3. SINGLE POINT BRUNAUER-EMMETT-TELLER (BET) SURFACE AREA, LANGMUIR SURFACE AREA, AND PORE VOLUME OF ACTIVATED CARBON (AC) AND COMMERCIAL ACTIVATED CARBON (CAC)

Sample	BET surface area ($m^2 g^{-1}$)	Micropore surface area ($m^2 g^{-1}$)	Total pore volume ($cm^3 g^{-1}$)	Micropore volume ($cm^3 g^{-1}$)
Raw PKS	0.7214	-	-	-
PKS AC	607.76	541.76	0.25	0.21
CAC	690.92	469.08	0.19	0.19

Note: PKS – palm kernel shell.

TABLE 4. COMPARISON OF THE MAXIMUM PERCENTAGE OF CHEMICAL OXYGEN DEMAND (COD) REMOVAL BY VARIOUS ADSORBENTS

Adsorbent types	Type of wastewater	COD removal (%)	Reference
Bagasse fly ash (BFA)	Pulp and paper	50	(Srivastava *et al*., 2005)
Powder activated carbon (PAC)	Refinery	72-92.5	(Hami *et al*., 2007)
Coconut fibres carbon (ATFAC)	Industrial (mixed)	50–74	(Mohan *et al*., 2008)
Rice husk carbon (ATRHC)	Industrial (mixed)	45–73	(Mohan *et al*., 2008)
Mixed adsorbent carbon (MAC)	Domestic	96	(Rani and Dahiya, 2008)
Bamboo-based activated carbon	Dyeing effluent from a cotton textile mill	75.21	(Ahmad and Hameed, 2009)
Electro-Fenton technology using an activated carbon fibre cathode	Dyeing	75.2	(Wang *et al*., 2010)
Bamboo waste activated carbon (BMAC)	Cotton textile mill	73.98	(Ahmad and Hameed, 2010)
Oil palm empty fruit bunches	POME	89	(Munirat, 2010)
Activated carbon fibre	Dyeing factory	75	(Aber and Sheydaei, 2012)
Lignite activated coke (LAC)	Super heavy oil wastewater (SHOW)	65.2	(Tong *et al*., 2014)
Palm kernel shell activated carbon	Palm oil mill effluent (POME)	80.7	This work

by various adsorbents reported in the literature. PKS AC used in this study showed comparable percentage of COD removal to those reported in other previous studies, and it is noteworthy that the prepared PKS AC was produced using commercial scale production while others were only at the laboratory scale.

Adsorption Isotherm

Adsorption isotherm is a graphical representation showing the quantity of adsorbate adsorbed by a unit of adsorbent. The most common models applied in examining the relationship between amounts of adsorbate adsorbed onto the adsorbent are Langmuir and Freundlich models. In this study, the linearised forms of Langmuir and Freundlich models were applied to fit the equilibrium data of adsorption of organics on the PKS and CAC.

Langmuir isotherm assumes monolayer adsorption onto a surface containing a finite number of adsorption sites of uniform approaches of adsorption with no transmigration of adsorbate in the plane of the surface (Weber and Chakravorti,

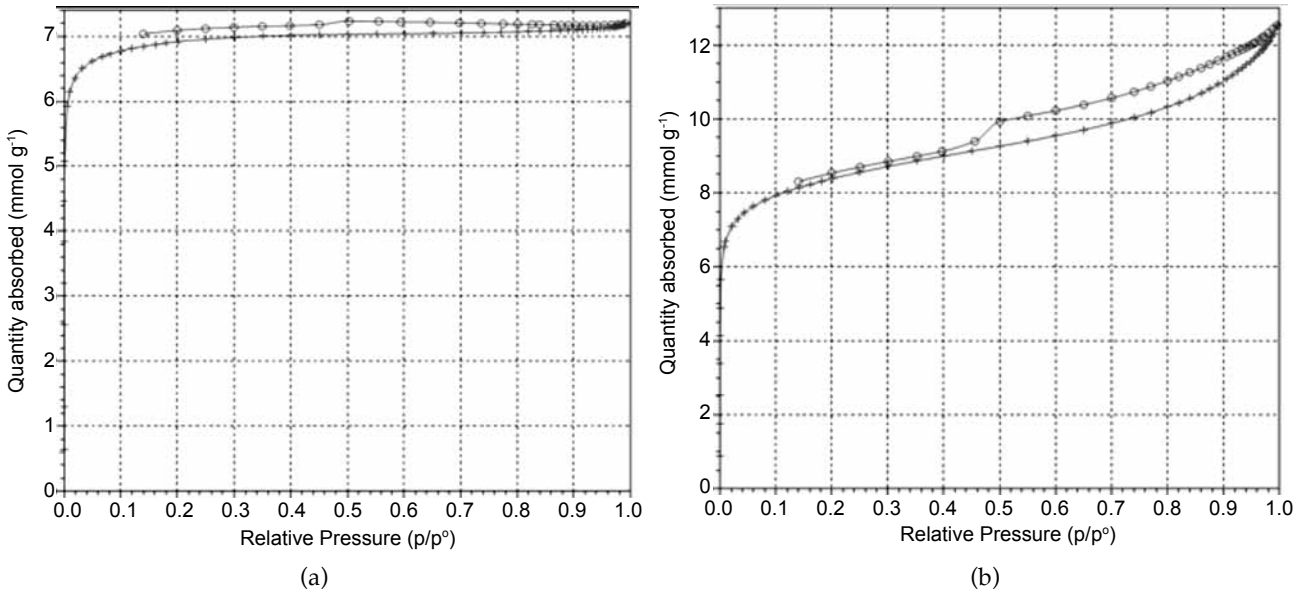

Figure 8. Nitrogen adsorption-desorption isotherm for: (a) palm kernel shell activated carbon (PKS AC) and (b) commercial activated carbon (CAC).

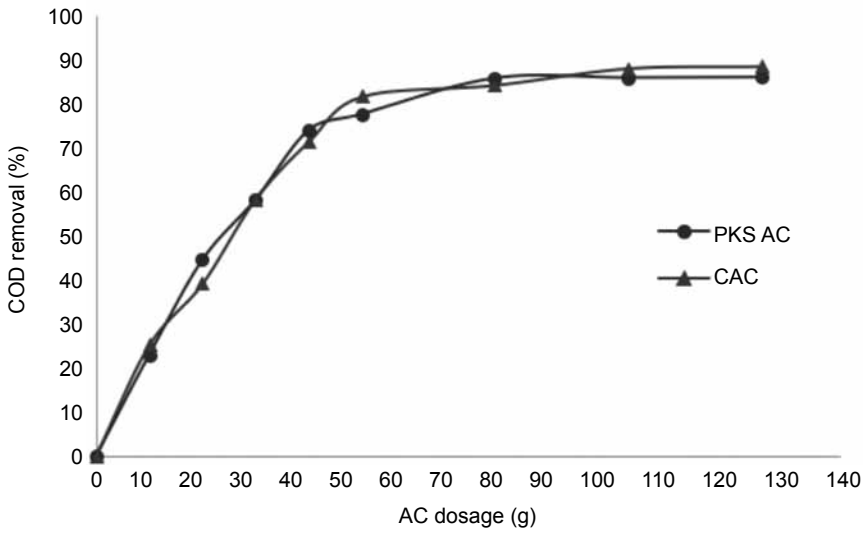

Figure 9. Effect of adsorbent dosage on chemical oxygen demand (COD) removal for palm kernel shell activated carbon (PKS AC) and commercial activated carbon (CAC).

1974). The linear form of Langmuir isotherm model equation is given by:

$$\frac{C_e}{q_e} = \frac{1}{K_L q_m} + \frac{1}{q_m} C_e \quad (3)$$

where Ce (mg litre^{-1}) is the residual COD concentration of aqueous solution; q_e (mg g^{-1}) is the amount of COD removed; K_L is the Langmuir constant; and q_m (mg g^{-1}) is the maximum adsorption capacity. The value of q_m and Langmuir constant can be obtained from the interception and the slope of C_e/q_e *vs*. Ce graph as shown in *Figure 10*.

The essential characteristics of Langmuir isotherm can be expressed by a dimensionless constant called equilibrium parameter, R_L as:

$$R_L = \frac{1}{1 + K_L C_O} \quad (4)$$

The parameter R_L indicates the shape of isotherm as follows:

Value of R_L	Type of isotherm
R_L >1	Unfavourable
a	Linear
0 < R_L < 1	Favourable
R_L =0	Irreversible

Another isotherm model that is usually employed is called Freundlich isotherm. This model is applied to describe the heterogeneity of the adsorbent adsorbate interaction and also suggests that sorption energy will exponentially decrease upon completion of the sorption centers of the adsorbent. Hence, the isotherm can be employed to describe the heterogeneous systems and having an empirical equation as follows:

$$q_e = K_f C_e^{\frac{1}{n}} \quad (5)$$

where q_e is the solid phase adsorbate concentration in equilibrium (mg g^{-1}), C_e is the equilibrium liquid phase concentration (mg L^{-1}), K_f is the Freundlich constant (L g^{-1}) related to bonding energy, also defined as adsorption coefficient and represents the quantity of the organics adsorbed onto adsorbent for unit equilibrium concentration. While 1/n is the heterogeneity factor and *n* is a measure of the deviation from linearity of the adsorption and its value represents the favourable of the adsorption isotherm (n>1). The well-known logarithmic form of Freundlich isotherm is given as:

$$\text{Log } q_e = \log K_f + 1/n \log C_e \quad (6)$$

Therefore, the constant K_f and the exponent 1/n can be obtained from a plot of $\ln q_e$ *vs*. $\ln C_e$. The Freundlich equation predicts that the organics concentration on the adsorbent will increase so long as there is an increase in the organic concentration in the POME solution. The linear plot of specific adsorption (C_e/q_e) *vs*. equilibrium concentration (C_e) for Langmuir model, and ($\ln q_e$) *vs*. ($\ln C_e$) for Freudlich model are clearly shown in *Figure 11*.

Table 5 summarises all the constants and correlation coefficient, R^2 values obtained from the two isotherm models employed for the adsorption of organic matter in POME for polishing treatment. It was observed that the equilibrium adsorption data for both PKS AC and CAC followed the Langmuir's adsorption isotherm since the correlation coefficient, R^2 is significantly higher than that of Freundlich

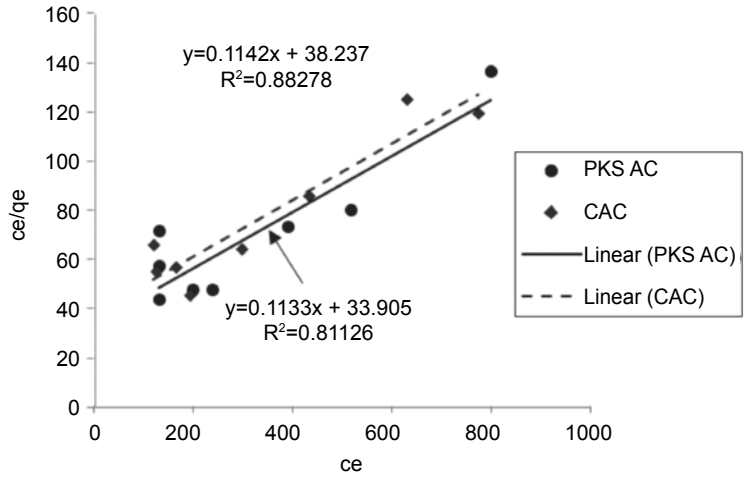

Figure 10. Langmuir isotherm plots for adsorption of organic matters onto palm kernel shell activated carbon (PKS AC) and commercial activated carbon (CAC) (adsorbent dosage = 50 g, agitation speed= 150 rpm, contact time = 24 hr, pH = 7.9).

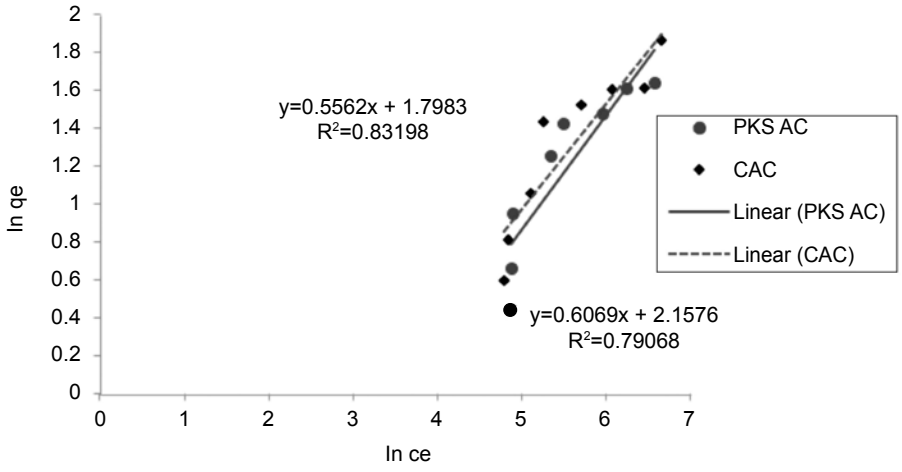

Figure 11. Freudlich isotherm plots for adsorption of organic matters onto palm kernel shell activated carbon (PKS AC) and commercial activated carbon (CAC) (adsorbent dosage = 50 g, agitation speed= 150 rpm, contact time = 24 hr, pH = 7.9).

TABLE 5. LANGMUIR, FREUNDLICH ISOTHERM CONSTANTS AND SEPARATION FACTORS (R_L) FOR ADSORPTION OF ORGANIC MATTER ON PALM KERNEL SHELL ACTIVATED CARBON (PKS AC) AND COMMERCIAL ACTIVATED CARBON (CAC)

AC sample	Langmuir isotherm			Freudlich isotherm			
	q_{max}	K_L	R_L	R^2	K_f	n	R^2
PKS AC	8.35	0.0028	0.28	0.81	0.12	1.65	0.80
CAC	8.76	0.0030	0.24	0.88	0.17	1.80	0.83

equation. This observation confirms the existence of monolayer adsorption of organic matter onto the internal and external surfaces of both ACs. *Table 5* shows the value of R_L for both PKS AC and CAC (0.28 and 0.24) are in the range of 0-1 which confirmed the favourable uptake of organic matter in POME. Therefore, the maximum adsorption amount of organic matter can be estimated to be 8.83 mg g^{-1} for PKS AC and 8.76 mg g^{-1} for CAC; these values are comparable. The result obtained indicated that the binding sites were distributed homogeneously over the external and internal surfaces of the prepared AC according to Langmuir assumption.

CONCLUSION

In this article, the PKS AC produced from the commercial carbonisation and activation plants were analysed and discussed. The BET surface area of the PKS AC is 607.76 m^2 g^{-1} (541.76 m^2 g^{-1} micropore surface area), which is comparable with the CAC available in the market with the BET surface area of 690.92 m^2 g^{-1} (469.08 m^2 g^{-1} micropore surface area). From SEM micrographs, the physically activated PKS showed well developed pores and clean surface compared to the raw PKS and PKS charcoal. This study also concludes that PKS can have a high potential as a source of AC due to low

ash content but high in volatile matter present in PKS. In addition, the performance of prepared PKS AC was examined by its ability to adsorb organic matter in POME polishing treatment in terms of COD reduction. The data were analysed by using Langmuir and Freudlich isotherm models, and fitted best to Langmuir isotherm confirming the formation of monolayer adsorbate to the surface of the adsorbent. This study supports earlier findings that in certain areas lignocellulosic agricultural residues can replace non-renewable resources, such as coal.

REFFERENCES

ABER, S and SHEYDAEI, M (2012). Removal of COD from industrial effluent containing indigo dye using adsorption method by activated carbon cloth: optimization, kinetic, and isotherm studies. *CLEAN – Soil, Air, Water, 40*: 87-94.

ACHAW, O-W and AFRANE, G (2008). The evolution of the pore structure of coconut shells during the preparation of coconut shell-based activated carbons. *Microporous and Mesoporous Materials, 112*: 284-290.

AHMAD, A A and HAMEED, B H (2009). Reduction of COD and color of dyeing effluent from a cotton textile mill by adsorption onto bamboo-based activated carbon. *J. Hazardous Materials, 172*: 1538-1543.

AHMAD, A A and HAMEED, B H (2010). Effect of preparation conditions of activated carbon from bamboo waste for real textile wastewater. *J. Hazardous Materials, 173*: 487-493.

AHMADPOUR, A and DO, D D (1997). The preparation of activated carbon from macadamia nutshell by chemical activation. *Carbon, 35*: 1723-1732.

ARRIAGADA, R; GARCÍA, R; MOLINA-SABIO, M and RODRIGUEZ-REINOSO, F (1997). Effect of steam activation on the porosity and chemical nature of activated carbons from Eucalyptus globulus and peach stones. *Microporous Materials, 8*: 123-130.

ASADULLAH, M; M A RAHMAN; M A MOTIN and M B SULTAN (2006). Preparation and adsorption studies of high specific surface area activated carbons obtained from the chemical activation of jute stick. *Adsorption Science Technology, 24*: 761.

ASTIMAR, A A; ROPANDI, M; NORFAIZAH, J; NAHRUL, H and ZAWAWI, I (2012). The production of oil palm based activated charcoal and pyroglineous acid (wood vinegar). *MPOB Information Series No. 515*.

BOUCHELTA, C; MEDJRAM, M S; BERTRAND, O and BELLAT, J -P (2008). Preparation and characterization of activated carbon from date stones by physical activation with steam. *J. Analytical and Applied Pyrolysis, 82*: 70-77.

CAO, Q; XIE, K-C; LV, Y-K and BAO, W-R (2006). Process effects on activated carbon with large specific surface area from corn cob. *Bioresource Technology, 97*: 110-115.

CHATTOPADHYAYA, G; MACDONALD, D G; BAKHSHI, N N; SOLTAN MOHAMMADZADEH, J S and DALAI, A K (2006). Preparation and characterization of chars and activated carbons from Saskatchewan lignite. *Fuel Processing Technology, 87*: 997-1006.

CHEN, X; JEYASEELAN, S and GRAHAM, N (2002). Physical and chemical properties study of the activated carbon made from sewage sludge. *Waste Management, 22*: 755-760.

CUERDA-CORREA, E M; MACÍAS-GARCÍA, A; DÍEZ, M A D and ORTIZ, A L (2008). Textural and morphological study of activated carbon fibers prepared from kenaf. *Microporous and Mesoporous Materials, 111*: 523-529.

DAUD, W M A W and ALI, W S W (2004). Comparison on pore development of activated carbon produced from palm shell and coconut shell. *Biosource Technology, 93*: 63-69.

DEIANA, C; GRANADOS, D; VENTURINI, R; AMAYA, A; SERGIO, M and TANCREDI, N (2008). Activated carbons obtained from rice husk: Influence of leaching on textural parameters. *Industrial & Engineering Chemistry Research, 47*: 4754-4757.

DEMIRBAŞ, A (1999). Properties of charcoal derived from hazelnut shell and the production of briquettes using pyrolytic oil. *Energy, 24*: 141-150.

DURÁN-VALLE, C J; GÓMEZ-CORZO, M; PASTOR-VILLEGAS, J and GÓMEZ-SERRANO, V (2005). Study of cherry stones as raw material in preparation of carbonaceous adsorbents. *J. Analytical and Applied Pyrolysis, 73*: 59-67.

ELIZALDE-GONZÁLEZ, M P and HERNÁNDEZ-MONTOYA, V (2007). Characterization of mango pit as raw material in the preparation of activated carbon for wastewater treatment. *Biochemical Engineering Journal, 36*: 230-238.

GARG, V K; GUPTA, R; BALA YADAV, A and KUMAR, R (2003). Dye removal from aqueous solution by adsorption on treated sawdust. *Bioresource Technology, 89*: 121-124.

GARG, V K; KUMAR, R and GUPTA, R (2004). Removal of malachite green dye from aqueous solution by adsorption using agro-industry waste: a case study of *Prosopis cineraria*. *Dyes and Pigments, 62*: 1-10.

GERÇEL, Ö; ÖZCAN, A; ÖZCAN, A S and GERÇEL, H F (2007). Preparation of activated carbon from a renewable bio-plant of *Euphorbia rigida* by H_2SO_4 activation and its adsorption behavior in aqueous solutions. *Applied Surface Science, 253*: 4843-4852.

GOMEZ-SERRANO, V; PASTOR-VILLEGAS, J; PEREZ-FLORINDO, A; DURAN-VALLE, C and VALENZUELA-CALAHORRO, C (1996). FT-IR study of rockrose and of char and activated carbon. *J. Analytical and Applied Pyrolysis, 36*: 71-80.

GUO, J and LUA, A C (2000). Preparation and characterization of adsorbents from oil palm fruit solid wastes. *J. Oil Palm Res. Vol. 12 No. 1*: 64-70.

GUO, J and LUA, A C (2003). Textural and chemical properties of adsorbent prepared from palm shell by phosphoric acid activation. *Materials Chemistry and Physics, 80*: 114-119.

HAMI, M L; AL-HASHIMI, M A and AL-DOORI, M M (2007). Effect of activated carbon on BOD and COD removal in a dissolved air flotation unit treating refinery wastewater. *Desalination, 216*: 116-122.

HU, Z; SRINIVASAN, M P and NI, Y (2001). Novel activation process for preparing highly microporous and mesoporous activated carbons. *Carbon, 39*: 877-886.

JIA, Q and LUA, A C (2008). Effects of pyrolysis conditions on the physical characteristics of oil-palm-shell activated carbons used in aqueous phase phenol adsorption. *J. Analytical and Applied Pyrolysis, 83*: 175-179.

JIBRIL, B Y; AL-MAAMARI, R S; HEGDE, G; AL-MANDHARY, N and HOUACHE, O (2007). Effects of feedstock pre-drying on carbonization of KOH-mixed bituminous coal in preparation of activated carbon. *J. Analytical and Applied Pyrolysis, 80*: 277-282.

LARTEY, R B; ACQUAH, F and NKETIA, K S (1999). Developing national capability for manufacture of activated carbon from agricultural wastes. *The Ghana Engineer*.

LI, D Y; H L ZHOU; Y J TIAN; L Q; WEI; X F WU; W J LI and Y F CHEN (2007). High specific surface area activated carbon from anthracite. *Rare Met. Material Engineering, 36*: 583.

LUA, A C and YANG, T (2005). Characteristics of activated carbon prepared from pistachio-nut shell by zinc chloride activation under nitrogen and vacuum conditions. *J. Colloid and Interface Science, 290*: 505-513.

MATOS, J; NAHAS, C; ROJAS, L and ROSALES, M (2011). Synthesis and characterization of activated carbon from sawdust of Algarroba wood. 1. Physical activation and pyrolysis. *J. Hazardous Materials, 196*: 360-369.

MATTSON, J S and MARK, H B (1971). *Activated Carbon: Surface Chemistry and Adsorption from Solution*. Marcel Dekker, New York.

MEIER, D; ANDERSONS, B; IRBE, I; CHIRKOVA, J and FAIX, O (2008). Preliminary study on fungicide and sorption effects of fast pyrolysis liquids used as wood preservative. *Progress in Thermochemical Biomass Conversion* (Bridgwater, A V ed.). Oxford: Blackwell Science. p. 1550-1563.

MOHAN, D; SINGH, K P and SINGH, V K (2008). Wastewater treatment using low cost activated carbons derived from agricultural byproducts - a case study. *J. Hazardous Materials, 152*: 1045-1053.

MORENO-CASTILLA, C; FERRO-GARCIA, M A; JOLY, J P; BAUTISTA-TOLEDO, I; CARRASCO-MARIN, F and RIVERA-UTRILLA, J (1995). Activated carbon surface modifications by nitric acid, hydrogen peroxide, and ammonium peroxydisulfate treatments. *Langmuir, 11*: 4386-4392.

MUNIRAT, A I (2010). Use of hybrid membrane system for the production of process water biologically treated palm oil mill effluent (POME). Unpublished Master dissertation, International Islamic University Malaysia, Kuala Lumpur.

MPOB (2013). http://bepi.mpob.gov.my, accessed on 25 April 2013.

NABAIS, J V; CARROTT, P; RIBEIRO CARROTT, M M L; LUZ, V and ORTIZ, A L (2008a). Influence of preparation conditions in the textural and chemical properties of activated carbons from a novel biomass precursor: The coffee endocarp. *Bioresource Technology, 99*: 7224-7231.

NABAIS, J M V; NUNES, P; CARROTT, P J M; RIBEIRO CARROTT, M M L; GARCÍA, A M and DÍAZ-DÍEZ, M A (2008b). Production of activated carbons from coffee endocarp by carbon dioxide and steam activation. *Fuel Processing Technology, 89*: 262-268.

NOLL, K E; DEMING, L S and HOU, W S (1992). *Adsorption Technology for Air and Water Pollution Control*. Michigan, Lewis. 25 pp.

OLIVARES-MARÍN, M; FERNÁNDEZ-GONZÁLEZ, C; MACÍAS-GARCÍA, A and GÓMEZ-SERRANO, V (2012). Preparation of activated carbon from cherry stones by physical activation in air. Influence of the chemical carbonisation with H_2SO_4. *J. Analytical and Applied Pyrolysis, 94*: 131-137.

PIETRZAK, R; WACHOWSKA, H; NOWICKI, P and BABEŁ, K (2007). Preparation of modified active carbon from brown coal by ammoxidation. *Fuel Processing Technology, 88*: 409-415.

RANI, D and DAHIYA, R P (2008). COD and BOD removal from domestic wastewater generated in decentralised sectors. *Bioresource Technology, 99*: 344-349.

RIOS, R V R A; MARTÍNEZ-ESCANDELL, M; MOLINA-SABIO, M and RODRÍGUEZ-REINOSO, F (2006). Carbon foam prepared by pyrolysis of olive stones under steam. *Carbon, 44*: 1448-1454.

RODRÍGUEZ-REINOSO, F; MOLINA-SABIO, M and GONZÁLEZ, M T (1995). The use of steam and CO_2 as activating agents in the preparation of activated carbons. *Carbon, 33*: 15-23.

ROUQUEROL, J; ROUQUEROL, F and SING, K S W (1998). *Adsorption by Powders and Porous Solids: Principles, Methodology and Applications*. Elsevier Science.

SJÖSTRÖM, E (1993). *Wood Chemistry: Fundamentals and Applications*. Chapter 10. Academic Press, San Diego. p. 234

SRIVASTAVA, V C; MALL, I D and MISHRA, I M (2005). Treatment of pulp and paper mill wastewaters with poly aluminium chloride and bagasse fly ash. *Colloids and Surfaces A: Physicochemical and Engineering Aspects, 260*: 17-28.

STAVROPOULOS, G G and ZABANIOTOU, A A (2005). Production and characterization of activated carbons from olive-seed waste residue. *Microporous and Mesoporous Materials, 82*: 79-85.

STUART, B H (2005). *Spectral Analysis. Infrared Spectroscopy: Fundamentals and Applications*. John Wiley & Sons, Ltd.

SUDARYANTO, Y; HARTONO, S B; IRAWATY, W; HINDARSO, H and ISMADJI, S (2006). High surface area activated carbon prepared from cassava peel by chemical activation. *Bioresource Technology, 97*: 734-739.

SUN, K and JIANG, J C (2010). Preparation and characterization of activated carbon from rubber-seed shell by physical activation with steam. *Biomass and Bioenergy, 34*: 539-544.

SUZUKI, R M; ANDRADE, A D; SOUSA, J C and ROLLEMBERG, M C (2007). Preparation and characterization of activated carbon from rice bran. *Bioresource Technology, 98*: 1985-1991.

TONG, K; ZHANG, Y; FU, D; MENG, X; AN, Q and CHU, P K (2014). Removal of organic pollutants from super heavy oil wastewater by lignite activated coke. *Colloids and Surfaces A: Physicochemical and Engineering Aspects, 447*: 120-130.

WANG, C -T; CHOU, W -L; CHUNG, M-H and KUO, Y-M (2010). COD removal from real dyeing wastewater by electro-Fenton technology using an activated carbon fiber cathode. *Desalination, 253*: 129-134.

WEBER, T W and CHAKRAVORTI, R K (1974). Pore and solid diffusion models for fixed-bed adsorbers. *AIChE Journal, 20*: 228-238.

YADAV, A K; ABBASSI, R; GUPTA, A and DADASHZADEH, M (2013). Removal of fluoride from aqueous solution and groundwater by wheat straw, sawdust and activated bagasse carbon of sugarcane. *Ecological Engineering, 52*: 211-218.